IEEE Access
Multidisciplinary | Rapid Review | Open Access Journal

Received December 28, 2021, accepted January 21, 2022, date of publication February 1, 2022, date of current version February 14, 2022.

Digital Object Identifier 10.1109/ACCESS.2022.3148426

Multibeam Doppler Sensor-Based Non-Contact Heartbeat Detection Using Beam Diversity

TSUKIKO KITAGAWA[1], (Graduate Student Member, IEEE), KOHEI YAMAMOTO[1], (Student Member, IEEE), KOJI ENDO[1], (Member, IEEE), AND TOMOAKI OHTSUKI[2], (Senior Member, IEEE)

[1]Graduate School of Science and Technology, Keio University, Yokohama-shi, Kanagawa 223-8522, Japan
[2]Department of Information and Computer Science, Keio University, Yokohama-shi, Kanagawa 223-8522, Japan

Corresponding author: Kohei Yamamoto (yamamoto@ohtsuki.ics.keio.ac.jp)

ABSTRACT Heartbeat detection could enable various applications in the medical and health care fields. In particular, non-contact heartbeat detection can be acceptable for those who have difficulty wearing devices, such as burn patients and infants. A Doppler sensor could be a key device to realize heartbeat detection without any wearable devices. Many researches in recent years have focused on heartbeat detection using a Doppler sensor with a single beam Doppler sensor. However, when the SNR (Signal-to-Noise Ratio) of heartbeat components is low for the beam direction, the heartbeat detection accuracy is likely to degrade. In this paper, for more accurate heartbeat detection, we propose a heartbeat detection method based on beam diversity using a multibeam Doppler sensor. Through the preliminary experiments, we clarified that the SNRs of heartbeat components differ from one beam to another. This means that when the SNR is low for one beam, the SNR could be high for the other beams. Inspired by this fact, the proposed method extracts heartbeat components from all peaks detected by the multi-beam signals. To verify the heartbeat detection accuracy of our method, we conducted the experiments for different detection ranges. The obtained results show that compared to the conventional methods using a single beam, our proposed method using multibeam detected heartbeat more accurately. This indicates the benefit of exploiting beam diversity, i.e., the heartbeat detection accuracy can be improved by utilizing beam diversity.

INDEX TERMS Health care, vital sign detection, heartbeat, RRI (R-R interval), multibeam Doppler sensor, spectrogram, beam diversity.

I. INTRODUCTION

Monitoring vital signs, such as heartbeat and respiration, is one of the essential technologies for understanding the state of human health. Hence, vital sign detection is in great demand for medical and home health care [1]–[6]. In particular, heartbeat detection is attracting much attention, because changes in RRI (R-R interval) and HR (Heart Rate) reflect heart disease and autonomic nervous system activity [7], [8]. Therefore, various heartbeat detection methods have been investigated extensively.

ECG (Electrocardiogram) and PPG (Photoplethysmography) are typical methods to detect heartbeats. However, these approaches have disadvantages such as limited mobility and discomfort for the patient caused by device attachment. In contrast, a radar has the potential to enable non-contact heartbeat detection, such as a Doppler sensor and ultrasound [9], [10]. In particular, thanks to the simple hardware architecture and small power consumption, a Doppler sensor-based heartbeat detection has been extensively studied. In the typical Doppler sensor-based heartbeat detection, a Doppler sensor transmits microwaves toward a subject's chest and then receives the microwaves reflected from the chest. By analyzing the Doppler-shifted received signal due to reflection, it is possible to capture chest movements caused by heartbeats. Based on this principle, a Doppler sensor has been used for not only heartbeat detection but also respiration and cough detection [11]–[13]. The Doppler sensor-based vital sign detection is highly demanded under the Covid-19 situation. Furthermore, the Doppler sensor-based heartbeat detection methods have another advantage that the subject can detect heartbeats while wearing clothes. Owing

The associate editor coordinating the review of this manuscript and approving it for publication was Filbert Juwono.

to these advantages, various heartbeat detection methods using a Doppler sensor have been proposed [14]–[29], [32]–[49].

The conventional methods use a Doppler sensor with only a single beam and detect heartbeat based on a received signal for the beam direction. However, compared to noise such as respiration and body movements, chest movements caused by heartbeat are significantly small. This means that when the SNR of heartbeat components over the received signal for the beam direction is low due to such noise, the heartbeat detection accuracy of the conventional methods tends to degrade. Therefore, it is highly demanded to develop a heartbeat detection method with robustness to the SNR degradation.

In this paper, we present a multibeam Doppler sensor-based non-contact heartbeat detection using beam diversity. The multibeam Doppler sensor-based heartbeat detection method has been proposed in our previous work [50]. In this work, through the preliminary experiments, we confirmed that the SNR of heartbeat components varies from one beam to another, indicating that even when the SNR is low in one beam, it could be high in other beams. Based on this fact, the method [50] uses the Viterbi algorithm to extract heartbeat components from all peaks detected by the multi-beam signals so that it could prevent missing heartbeats due to SNR degradation. Here, it is worth mentioning that the difference between this paper and [50] is that this paper provides more detailed evaluation of the proposed method. Specifically, we give the performance evaluation of our method for different parameter settings, the performance evaluation to emphasize the benefit of using beam diversity. In particular, by evaluating the performance for three parameters, we achieve better accuracy than [50]. Furthermore, we present the performance comparison between the proposed and the existing heartbeat detection methods.

The rest of this paper is organized as follows. In Section II, we describe the principle of a multibeam Doppler sensor and then explain some related work in Section III. In Section IV, we explain our proposed method. We evaluate the performance of our method experimentally in Section V. Finally, we conclude this paper in Section VI.

II. FUNDAMENTAL PRINCIPLE OF MULTIBEAM DOPPLER SENSOR

In this section, we explain the principle of the multibeam Doppler sensor. Fig. 1 illustrates the system model of heartbeat detection using a multibeam Doppler sensor. The used multibeam Doppler sensor consists of one transmit antenna and four receive antennas. In this system, microwaves $T(t) = \cos(2\pi ft + \Phi(t))$ are firstly transmitted from the transmit antenna Tx towards a subject. Here, f and $\Phi(t)$ represent the carrier frequency and the phase noise, respectively. When the transmitted microwaves are reflected by the subject's body, the phase of $T(t)$ is Doppler-shifted. The reflected microwaves are then received by the receive antennas Rx k. Now, let $R_k(t)$ denote the received signal at the k th receive

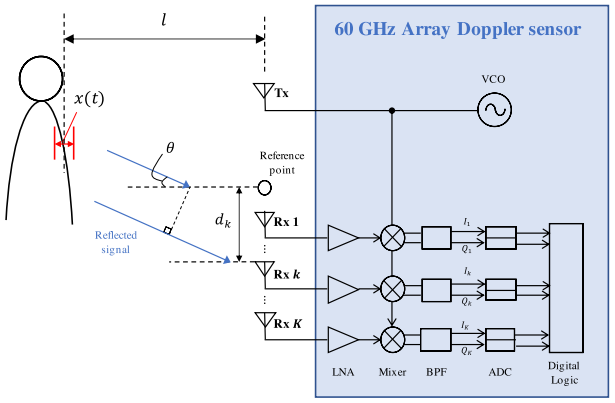

FIGURE 1. The system model.

antenna. The received signal $R_k(t)$ is expressed as

$$R_k(t) = \cos\Big(2\pi ft - \frac{4\pi l}{\lambda} - \frac{4\pi x(t)}{\lambda} + \Phi\Big(t - \frac{2l}{c}\Big) + \frac{2\pi}{\lambda} d_k \sin\theta\Big) \quad (1)$$

where c is the speed of the electromagnetic wave, λ is the wavelength of the carrier, l is the distance between the Doppler sensor and the subject, and $x(t)$ is the variation of l due to heartbeats. Using a quadrature mixer, in-phase and quadrature signals $I_k(t)$ and $Q_k(t)$ are obtained as follows.

$$I_k(t) = \cos\Big(\theta_c + \frac{\pi}{4} + \frac{4\pi x(t)}{\lambda} + \Delta\Phi(t) + \frac{2\pi}{\lambda} d_k \sin\theta\Big), \quad (2)$$

$$Q_k(t) = \cos\Big(\theta_c - \frac{\pi}{4} + \frac{4\pi x(t)}{\lambda} + \Delta\Phi(t) + \frac{2\pi}{\lambda} d_k \sin\theta\Big), \quad (3)$$

where θ_c is the constant phase. By beamforming, we can obtain $I_\theta(t)$ and $Q_\theta(t)$ for a specific beam direction. $I_\theta(t)$ and $Q_\theta(t)$ can be described by a complex signal $S_\theta(t)$, which is referred to as a Doppler signal.

$$S_\theta(t) = I_\theta(t) + jQ_\theta(t) \quad (4)$$

Through DSP (Digital Signal Processing), the proposed heartbeat detection is performed based on the Doppler signal $S_\theta(t)$ for multiple beam directions.

III. RELATED WORK

In this section, we explain existing researches related to Doppler sensor-based heartbeat detection. Heartbeat detection can be basically categorized into (i) HR estimation and (ii) RRI estimation. On the one hand, the conventional methods estimate the HR leveraging the time-frequency analysis such as

- FFT (Fast Fourier Transform) [14]–[18]
- WT (Wavelet Transform) [19]–[23]
- MUSIC (Multiple Signal Classification) [24]–[27]
- DCT (Discrete Cosine Transform) [28]

FFT is a typical technique used for analyzing the periodicity of a signal. In general, the normal respiration rate varies

between 0.1 Hz and 0.3 Hz, while the normal HR ranges between 0.5 Hz and 2 Hz. Based on this fact, by applying FFT to the received signal of a Doppler radar, the conventional methods separate the frequency components of heartbeats from those of respiration [14]–[16]. However, the SNR of heartbeat components is low, compared to that of respiration. Thus, extracting frequency components of heartbeats could be challenging due to respiration harmonics. The conventional method has introduced a method to reduce the effect of respiration harmonics [17]. However, to estimate the heart rate, a time window longer than 8 s is generally required to achieve a high-frequency resolution. This means that the HR can vary within a time window and it is impossible to estimate short-term HR changes [14]–[16], e.g., HR changes within 5 s. To deal with this issue, Tu and Lin have proposed HR estimation with a time window shorter than 5 s [18]. However, these conventional methods still have the issue related to the degradation of the HR estimation accuracy due to body movements.

As one of the techniques to analyze the periodicity of a signal, WT has also been used in the field of the Doppler radar-based heart rate estimation method [19]–[23]. WT analyzes the periodicity of a signal by scaling and shifting the prototype signal called the mother wavelet, and provides high time-frequency resolution, compared to FFT. In the WT-based HR estimation method, the HR is estimated by estimating a scale factor. The experimental results have shown that compared to the FFT-based method, the conventional methods [19]–[22] could provide more accurate HR even with a time window shorter than 8 s. However, to estimate short-term HR changes, the time windows used in these conventional methods are long. To address this problem, Li and Lin have proposed the HR estimation method with a shorter time window that is adaptively set [23]. Basically, there are many choices of the prototype signal, and a suitable selection of the prototype signal brings the accurate heart rate estimation. However, nonheartbeat, e.g., respiration and body movements, could deform heartbeat signal waveforms, which changes the suitable prototype signal to estimate the heart rate. Also, HR estimation accuracy tends to degrade due to body movements.

In addition to FFT and WT, the MUSIC algorithm has also been investigated for the heart rate estimation [24]–[27]. Bechet *et al.* have shown the feasibility of the MUSIC algorithm-based heart rate estimation; the MUSIC algorithm provided the accurate heart rate, compared to FFT [24]. However, to estimate the heart rate by the MUSIC algorithm, it is necessary to estimate the number of the sinusoidal signals composing the analyzed signal. Thus, Kwang *et al.* have proposed the method that tracks the fundamental and harmonic frequencies of heartbeats over the MUSIC spectrum, and then estimates the heart rate by judging whether at least one of the MUSIC spectrum peaks in the current window appear at the frequencies with the peaks in the previous window [25]. However, this conventional method requires a long time window, i.e., a 60 s-time window, so that peaks due to heartbeat appear over the MUSIC spectrum even in the presence of the noise. Thus, as aforementioned, it is impossible to estimate the small heart rate variability, e.g., the variability within 5 s. To deal with this problem, the work [26] has proposed a MUSIC algorithm-based heart rate estimation method with a 5 s-time window. The experimental results showed this method achieved the high heart rate estimation accuracy, compared with the conventional one [25]. However, when the heart rate changes largely even within the 5 s-time window, several peaks due to heartbeats appear over the MUSIC spectrum, which might cause incorrect peak detection. Such occurrence of several peaks is due to the fixed window size. Thus, in the conventional method [27], the adaptive window size setting technique has been incorporated into the method [26] to prevent such incorrect peak detection. However, there is still an issue related to the degradation of the HR estimation accuracy due to body movements.

Also, the previous research [28] has investigated the HR estimation method based on DCT, which has been used for image compression. The conventional method [28] has been shown to achieve a higher HR estimation accuracy even with a short time window than the FFT-based methods. On the contrary, the HR estimation accuracy is likely to degrade due to respiration and body movements. In addition to these HR estimation methods, Nosrati and Tavassolian have introduced the FTPR (Frequency Time Phase Regression) algorithm for the accurate HR estimation [29]. However, this method requires a long time window, i.e., 10 s. While a number of HR estimation methods based on FFT, WT, and MUSIC have been studied, [30] and [31] are also used as spectral estimation, and could be applied for HR estimation.

On the other hand, in the Doppler radar-based RRI estimation, the RRI can be estimated by the template matching algorithm [32]–[35] and the feature detection [36]–[48]. The template matching-based methods prepare a template waveform of a heartbeat in advance and then detect heartbeats by comparing the received signal with the prepared template waveform [32]–[34]. The conventional methods [32]–[34] could estimate the RRI accurately by using novel peak detection algorithms over the signal obtained through some signal processing. However, heartbeat signal waveforms could change over time and it is challenging to prepare ideal template waveforms. This is because heartbeat signal waveforms are likely to be distorted by noise such as respiration and body movements. Although the conventional method [35] could estimate the RRI with the robustness to distortion of a heartbeat signal waveform, an RRI estimation accuracy tends to degrade in the situation where the SNR of heartbeat components is low.

In contrast, the feature detection-based RRI estimation method detects heartbeat by extracting features due to a heartbeat from the received signal. Many conventional methods extract peaks from heartbeat signal waveforms as a feature [36]–[42]. These conventional methods could estimate the RRI accurately by using novel peak detection

algorithms over the signal obtained through some signal processing, such as a Band Pass Filter (BPF). However, when the SNR of heartbeat components is low, many incorrect peaks could appear over the signal even after some processing, which could degrade a peak detection accuracy. Furthermore, the conventional methods [43]–[46] could extract a heartbeat signal through some advanced signal processing, e.g., WT and EEMD (Ensemble empirical mode decomposition), which could reduce peak candidates and bring accurate peak detection over the heartbeat signal. Although Sakamoto *et al.* have proposed the feature-based correlation method by extreme points and inflection points of the received signal [46], the heartbeat detection accuracy is likely to degrade as well as the conventional method. Hu *et al.* have proposed the method that estimates the RRI based on zero crossings of the time-domain signal obtained through various signal processing, e.g., WT and EEMD [47]. EEMD can decompose the analyzed signal to some components called IMF (Intrinsic Mode Function) with different frequency components. The conventional method [47] reconstructs a heartbeat signal based on some IMFs, and detects heartbeat by capturing zero-crossing points of the reconstructed signal. However, it is challenging to select appropriate IMFs for heartbeat signal reconstruction. Also, when the SNR of heartbeat components is low, many incorrect zero-crossing points could appear over the signal even after some processing, which could degrade a zero-crossing detection accuracy. Petrovic *et al.* have proposed a heartbeat detection method that first estimates a rough HR, and then designs a narrow BPF with the estimated rough HR as the center frequency [48]. This method then applies the narrow BPF to the signal obtained from a received signal of a Doppler radar and detects heartbeat by the zero-crossings of the selected BPF output. Although the experimental results show that this method can provide an accurate heartbeat detection accuracy as long as the SNR of heartbeat components is high, it is still challenging to detect heartbeat accurately with robustness to low SNR.

Based on the above discussion, the heartbeat detection accuracy tends to degrade, when the SNR of heartbeat components is low. In these conventional methods, a Doppler sensor with one beam is used, meaning that only the received signal for one beam direction is used to detect heartbeats. Therefore, when the SNR of heartbeat components is low for the beam direction, it is challenging to detect heartbeat accurately.

IV. PROPOSED METHOD

In this section, we propose a multibeam Doppler sensor-based non-contact heartbeat detection using beam diversity. We first explain the idea of the proposed method and then explain the algorithm in detail.

A. IDEA OF PROPOSED METHOD

To clarify the connection between the SNR of heartbeat components and the beam direction, we conducted the preliminary experiments using a multibeam Doppler sensor to observe heartbeats from a sitting subject. Fig. 2 shows the integrated spectrum for different beam directions, i.e., $-40°$, $-20°$, $0°$, $20°$, and $40°$. In this figure, the amplitude of each signal is scaled. From Fig. 2, it can be seen that even when the peak due to heartbeat does not appear over one beam direction, the peak could appear over the other ones. Specifically, at 72 s, the peak due to heartbeat does not appear over the signal for $-20°$ and $0°$, while the peak appears over the signals for other directions. Also, we can see the same phenomenon at about 77 s. These are because the region of interest is different from one beam direction to another. Based on this fact, even when the SNR of heartbeat components gets low for some beam directions, it could be possible to prevent the degradation of the heartbeat detection accuracy by utilizing the diversity of the signals for various beam directions.

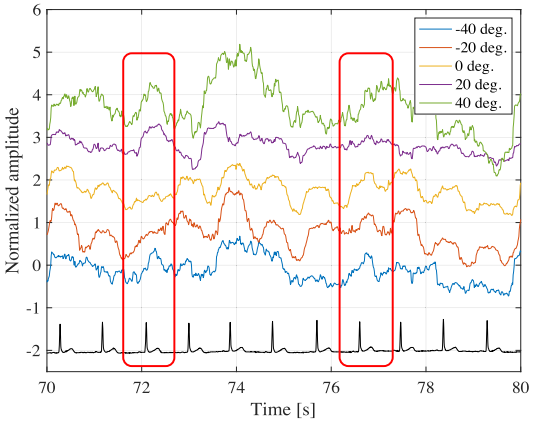

FIGURE 2. The integrated spectrum for different beam directions.

B. ALGORITHM

Fig. 3 shows the flowchart of the proposed method.

1) PRE-PROCESSING

First, the Doppler signal $S_\theta(t)$ for each beam direction θ at time t is acquired by beamforming every $\theta_b°$. After acquiring the Doppler signal $S(t)$, BPF is then applied to each Doppler signal to reduce the effect of non-heartbeat components. The cut-off frequencies of the BPF are set to 5.0 Hz and 30 Hz [49]. STFT is subsequently applied to each filtered signal. The time window size and its step size are set to 512 ms and 10 ms, respectively, and these parameters are sufficient to analyze the spectrum due to one heartbeat. Afterward, the spectrum within [5.0, 30] Hz and $[-30, -5.0]$ Hz are integrated, which brings the integrated spectrum $E(t)$ as shown in Fig. 2.

2) PEAK DETECTION BY USING THE VITERBI ALGORITHM

To reduce the effect of the undesired peaks due to noise, BPF is applied to $E(t)$ for each beam direction, where the cut-off frequencies are set to 0.8 Hz and 2.0 Hz corresponding to 48 bpm (beat per minute) and 120 bpm, respectively. Peaks

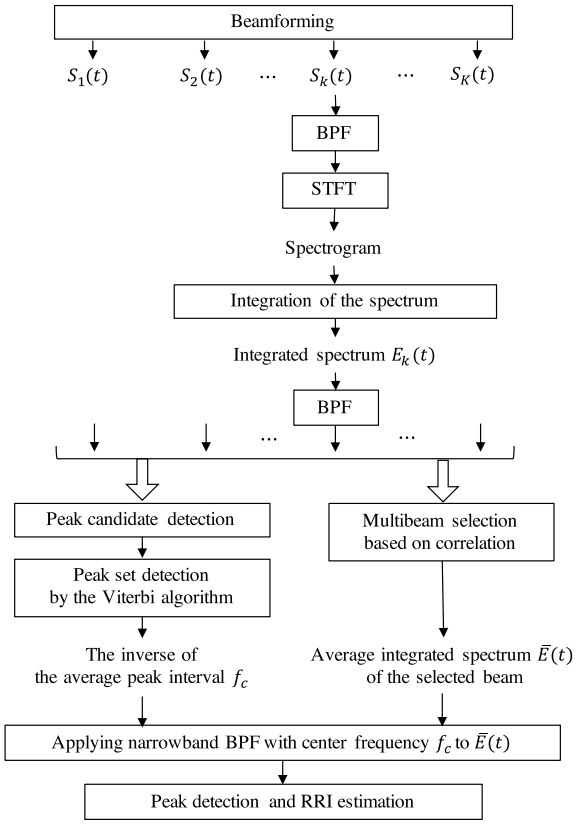

FIGURE 3. The flowchart of the proposed method.

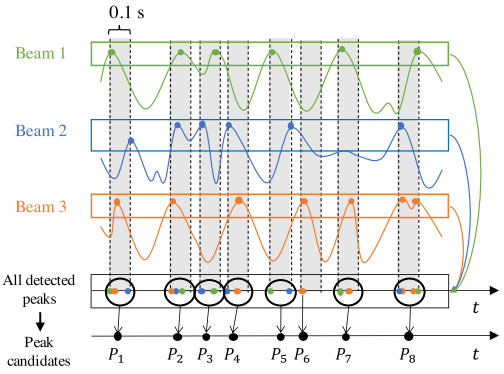

FIGURE 4. The concept of peak candidate detection.

of the filtered $E(t)$ for each beam direction are detected. The detected peaks are the peak candidates that might be caused by heartbeat, and thus heartbeat could be detected by selecting correct peaks over the peak candidates. Also, as aforementioned in Section IV. A, the use of various beam directions can lead to the prevention of missing heartbeat. In the proposed method, multiple peaks occurring within 0.1 s are regarded as one peak candidate, and the average of the time at which each peak occurs within 0.1 s is set up at the time when the peak occurs. Fig. 4 shows the concept of peak candidate detection. In this figure, 19 peaks are detected for three-beam directions, and then 8 peak candidates, i.e., $P_1, \ldots, P_8$, are obtained by combining the peaks occurring within 0.1 s. To select the most reliable peaks from the peak candidates, the Viterbi algorithm is used. The Viterbi algorithm estimates the most reliable sequence by using a predefined metric which is called a branch metric. Now, we define a set of RRIs as $\mathbf{B} = \{RRI_1, RRI_2, \ldots, RRI_M\}$, where M is the number of observed RRIs. Also, we let S_m denote the difference between two adjacent RRIs, i.e., $S_m = |RRI_{m+1} - RRI_m|$, and we define a set of S_m as $\mathbf{X} = \{S_1, S_2, \ldots, S_{M-1}\}$. Based on the fact that the difference between two adjacent RRIs follows the Gaussian distribution with zero mean, we can express the probability distribution of S_m as the following equation [41].

$$P(S_m) = \frac{1}{\sqrt{2\pi\sigma^2}} \exp -(S_m^2/2\sigma^2), \tag{5}$$

where σ^2 is a variance of S_m. The Viterbi algorithm estimates a combination of $\mathbf{X}$ with a maximum likelihood as

$$\hat{\mathbf{X}} = \arg\max_{\mathbf{X}} P(\mathbf{X}) = \arg\max_{\mathbf{X}} \prod_{m=1}^{M-1} P(S_m). \tag{6}$$

Also, we can rewrite eq. (6) using a log likelihood function.

$$\hat{\mathbf{X}} = \arg\max_{\mathbf{X}} \ln \prod_{m=1}^{M-1} P(S_m) = \arg\max_{\mathbf{X}} \sum_{m=1}^{M-1} \ln P(S_m). \tag{7}$$

Based on eqs. (5) and (7), we finally obtain eq. (4).

$$\hat{\mathbf{X}} = \arg\max_{\mathbf{X}} \sum_{m=1}^{M-1} -S_m^2 = \arg\min_{\mathbf{X}} \sum_{m=1}^{M-1} S_m^2. \tag{8}$$

According to the above equation, we can obtain a set of S_m with a maximum likelihood by minimizing the sum of S_m^2, which indicates that S_m^2, i.e., the squared difference between two adjacent RRIs, can be used as the branch metric.

3) IMPROVEMENT OF RRI ESTIMATION ACCURACY BASED ON NARROW BPF

After applying the Viterbi algorithm, the RRI can be estimated by calculating the interval of the selected peaks. However, one heartbeat sometimes causes multiple peaks, which could make some errors between the estimated and actual RRIs. To deal with this issue, the proposed method uses a narrow BPF so that only one peak appears for one heartbeat. The center frequency of the narrow BPF, f_c, is calculated as the reciprocal of the average interval of the selected peaks. In the experiments, since the subject's state is static, we assume that the HR does not largely change. Therefore, all the peaks selected during the observation duration of 2 minutes are used to calculate the center frequency f_c. The RRI is estimated by detecting peaks over the signal filtered by the narrow BPF. As the signal to which the narrow BPF is applied, the signals for multiple beam directions should be used to reduce the effects of the undetected heartbeat. However, since the timing of the heartbeat peak

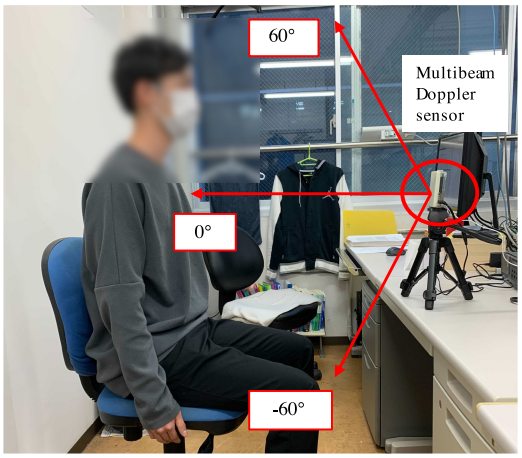

FIGURE 5. The experimental environment.

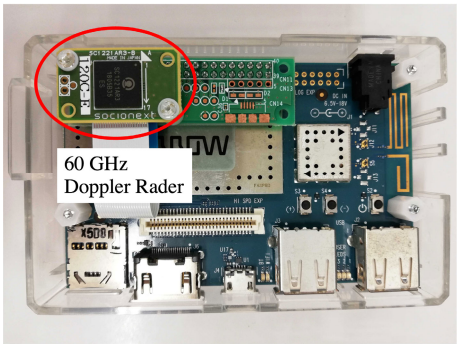

FIGURE 6. 60 GHz doppler radar.

is slightly different from one beam direction to another, the use of more beam directions could lead to a larger error between the estimated and actual RRIs. Therefore, the proposed method picks up the beam directions that have the integrated spectrum that is highly correlated with the integrated spectrum for the beam direction 0°. Specifically, the correlation coefficients among the integrated spectrums for 0° and the other beam directions are calculated every T_c seconds. The beam direction is then selected when the correlation coefficient for the beam direction exceeds a threshold th_c. After the beam selection, the average integrated spectrum for the selected beam directions, $\bar{E}(t)$, is calculated, and the narrow BPF is applied to $\bar{E}(t)$.

V. PERFORMANCE EVALUATION

In this section, we first explain the evaluation specification and then show the results.

A. EVALUATION SPECIFICATION

To show the heartbeat detection accuracy of the proposed method, we performed the experiments and calculated the AE (Absolute Error) between the estimated and ground-truth center frequencies of the narrow BPF, i.e., f_c.

$$AE = |f_{c_{est}} - f_{c_{ref}}|, \tag{9}$$

TABLE 1. The experimental specification.

Item	Value
The number of transmit antennas	1
The number of receive antennas	4
Carrier frequency	60 GHz
Sampling rate of multibeam Doppler sensor	1000 Hz
Distance between the multibeam Doppler sensor and a subject	0.6 m, 1.0 m, 2.0 m, and 3.0 m
The number of subjects	5
Observation duration	2 min
Beamforming range	From $-60°$ to $60°$
Bandwidth of the narrow BPF	0.3 Hz

where $f_{c_{est}}$ and $f_{c_{ref}}$ are the estimated and ground truth center frequencies, respectively. Moreover, as a performance metric of the RRI estimation accuracy, we calculated the RMSE (Root Mean Squared Error) between the estimated and ground-truth RRIs.

$$RMSE = \sqrt{\frac{1}{M}\sum_{m=1}^{M} |RRI_{est}(m) - RRI_{ref}(m)|^2}, \tag{10}$$

where M is the number of observed RRIs, $RRI_{est}(m)$ and $RRI_{ref}(m)$ are the m th estimated and ground-truth RRIs, respectively. We also show the CDF (Cumulative Distribution Function) of all the subjects as an evaluation index, which is a function of the probability that the error between the estimated and ground-truth RRIs X is less than or equal to x. It is expressed by the following equation.

$$F_X(x) = P(X \leq x), \tag{11}$$

Fig. 6 shows the experimental environment and TABLE 1 lists the experimental specification. A Doppler sensor can be realized with simple hardware and small power consumption, compared to an FMCW radar. Thus, we used a 60 GHz multibeam Doppler sensor with a sampling rate of 1000 Hz from Socionext Inc., SC1221AR3. The size of the sensor module is 9.0 mm × 9.0 mm, and the desired detection range is a frontal distance of 10 m and a detectable angle width of 120°. In the experiments, the heartbeat was observed from each subject sitting still with natural breathing. The detection range, i.e., the distance between the multibeam Doppler sensor and the subject's chest, was 0.6 m, 1.0 m, 2.0 m, and 3.0 m. The observation was performed on 5 healthy subjects (all male, aged 20s). Each observation duration was 2 minutes and the data were processed offline with MATLAB. The ground truth timings of the heartbeat were observed by ECG. Also, in this experiment, the angles considered for beamforming ranged from $-60°$ to 60°, which covers from the subject's head to his/her thigh. In order to reduce the effect

TABLE 2. The RRI estimation accuracy performance comparison of the proposed method∗ for different beam intervals between adjacent directions.

θ_b [°]	0.6 m		1.0 m		2.0 m		3.0 m		Ave.	
	AE [Hz]	RMSE [ms]	AE [Hz]	RMSE [ms]	AE [Hz]	RMSE [ms]	AE [Hz]	RMSE [ms]	AE [Hz]	RMSE [ms]
3	0.069	76	0.064	108	0.068	124	0.088	139	0.072	112
5	0.047	63	0.045	103	0.070	118	0.084	137	0.062	105
10	0.050	72	0.057	104	0.066	120	0.079	124	0.063	105
15	0.050	85	0.073	115	0.078	129	0.085	133	0.072	115
20	0.055	93	0.075	116	0.073	129	0.068	125	0.068	116
30	0.065	106	0.089	121	0.073	125	0.082	134	0.077	122
Ave.	0.056	82	0.067	111	0.071	124	0.081	132	0.069	112

∗ The proposed method uses the time interval T_c of 30 s, the threshold th_c of 0.9.

TABLE 3. The RRI estimation accuracy performance comparison of the proposed method∗ for different time intervals T_c.

T_c	RMSE [ms]				
	0.6 m	1.0 m	2.0 m	3.0 m	Ave.
5	96	91	138	138	116
10	75	103	123	137	109
15	69	103	121	139	108
20	65	105	123	144	109
30	63	103	118	138	105
60	61	99	126	138	106
120	62	98	127	137	106
Ave.	70	100	125	139	109

∗ The proposed method uses the beam interval between adjacent directions θ_b of 5°, the threshold th_c of 0.9.

TABLE 4. The RRI estimation accuracy performance comparison of the proposed method∗ for different thresholds th_c.

th_c	RMSE [ms]					Average number of the used beams
	0.6 m	1.0 m	2.0 m	3.0 m	Ave.	
None	87	108	129	133	114	25
0.1	88	107	129	133	114	25
0.2	87	106	129	133	114	25
0.3	86	107	130	133	114	25
0.4	85	108	130	133	114	23
0.5	81	106	129	133	112	22
0.6	81	106	129	135	113	18
0.7	78	104	127	135	111	14
0.8	76	102	124	140	111	10
0.9	75	103	123	137	109	6
Ave.	82	106	128	135	113	-

∗ The proposed method uses the beam interval between adjacent directions θ_b of 5°, the time interval T_c of 30 s.

of noise caused by body movements, it could be better to limit the beamforming range to the chest area and use fewer beams to detect heartbeat. However, since a multi-beam Doppler sensor is used for heartbeat detection for the first time, the beamforming range is set widely to explore which beam range should be used for heartbeat detection. The bandwidth of the narrow BPF was set to 0.3 Hz.

B. HEARTBEAT DETECTION ACCURACY

First, we discuss three parameters: (i) the beam interval θ_b, (ii) the time duration for calculating correlation coefficient T_c, and (iii) the correlation coefficient threshold th_c. TABLE 2 lists the AE and the RMSE of the proposed method for different beam intervals θ_b when T_c and th_c are set to 30 s and 0.9, respectively. Here, note that these parameters T_c and th_c are discussed later. When $\theta_b = 30°$, which means that the proposed method uses the beam directions from $-60°$ to 60° by 30°, i.e., $-60°$, $-30°$, 0°, 30°, and 60°. From this table, it can be seen that as the used beam interval θ_b is smaller, the AE and the RMSE are smaller except for the case of $\theta_b = 3°$. This is because using more beams gives more peak candidates, and the Viterbi algorithm can estimate the center frequency of the narrow BPF more accurately. However, it is also found that when θ_b is 3°, too many peak candidates occur, which degrades the peak detection accuracy of the Viterbi algorithm. TABLE 3 shows the RMSE of the proposed method for different time intervals T_c, where θ_b and th_c are set to 5° and 0.9, respectively. In this table, it can be seen that the RMSE becomes smaller as the time interval T_c becomes larger. This result indicates that the effect of the temporary degradation of the SNR can be reduced by taking the time interval T_c longer. TABLE 4 lists the RMSE of the proposed method for different correlation coefficient thresholds th_c, where θ_b and T_c are set to 5° and 30 s, respectively. As can be seen from this table, the RMSE becomes smaller as the threshold th_c becomes larger. This is because the smaller threshold leads to the more integrated spectrum where noise components may exist. We can also say that when the threshold exceeds 0.7, the RMSEs for the

TABLE 5. The RRI estimation accuracy performance comparison of the proposed methods that use multibeam and a single beam.

Single Beam	0.6 m		1.0 m		2.0 m		3.0 m		Ave.	
Direction [$^\circ$]	AE [Hz]	RMSE [ms]	AE [Hz]	RMSE [ms]	AE [Hz]	RMSE [ms]	AE [Hz]	RMSE [ms]	AE [Hz]	RMSE [ms]
60	0.091	142	0.130	192	0.142	203	0.135	184	0.124	180
50	0.091	145	0.127	187	0.143	202	0.136	190	0.124	181
40	0.083	147	0.141	198	0.144	199	0.135	187	0.126	183
30	0.089	129	0.151	204	0.131	188	0.136	185	0.127	176
20	0.079	122	0.140	204	0.128	186	0.133	181	0.120	173
10	0.080	127	0.123	169	0.131	187	0.137	184	0.118	167
0	0.095	142	0.122	162	0.137	180	0.137	186	0.123	167
-10	0.089	125	0.129	183	0.125	184	0.131	185	0.118	169
-20	0.106	161	0.134	189	0.128	184	0.128	179	0.124	178
-30	0.087	146	0.142	193	0.138	182	0.138	192	0.126	178
-40	0.087	140	0.134	199	0.125	180	0.121	175	0.117	174
-50	0.081	143	0.137	195	0.134	185	0.133	187	0.121	177
-60	0.084	155	0.131	186	0.136	186	0.129	184	0.120	178
Ave.	0.088	140	0.134	189	0.134	188	0.133	185	0.122	176
Proposal*	0.047	63	0.045	103	0.070	118	0.084	138	0.062	105

$*$ The proposed method uses the beam interval between adjacent directions θ_b of 5°, the time interval T_c of 30 s and the threshold th_c of 0.9.

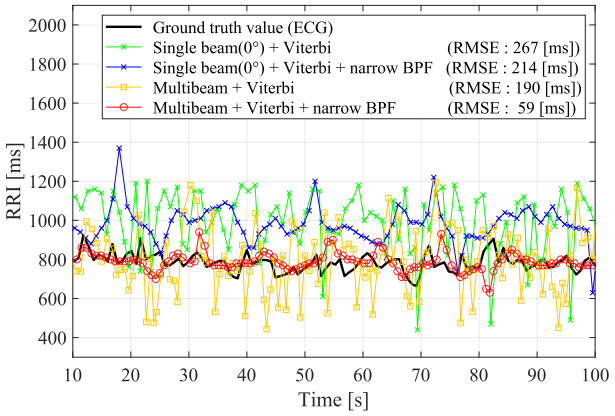

FIGURE 7. An example of the ground truth RRIs, the RRIs estimated by the Viterbi algorithm and the RRIs estimated by the Viterbi algorithm and narrow BPF when using the single beam of 0°, and the RRIs estimated by the Viterbi algorithm and the RRIs estimated by the Viterbi algorithm and narrow BPF when using the proposed method at the measurement distance of 0.6 m.

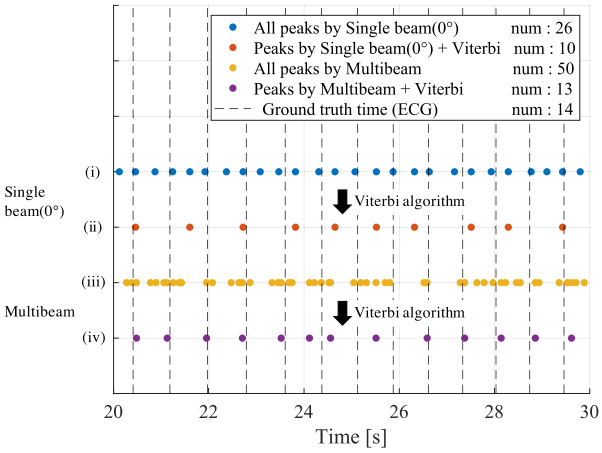

FIGURE 8. An example of peak detection. From the top, (i) all the peaks detected after peak candidate detection and (ii) estimated after Viterbi when using the single beam of 0°, and (iii) all the peaks detected after peak candidate detection and (iv) estimated after Viterbi when using the proposed method are shown. The dotted line shows the correct timing of the peaks obtained by ECG. Also, 'num' is the number of peaks detected in 10 seconds.

corresponding thresholds are similar to each other, which indicates that the thresholds that exceed 0.7 bring the similar integrated spectrum that could prevent missing heartbeat. As a result, the best accuracy is obtained with $\theta_b = 5^\circ$, $T_c = 30\ s$, and $th_c = 0.9$, which is used in the following discussion.

C. BENEFIT OF BEAM DIVERSITY

Based on the previous results, we set the beam interval θ_b, the time width for the correlation calculation T_c, and the correlation coefficient threshold th_c to 5°, 30 s, and 0.9, respectively. First, we compare the performance of the proposed method using multibeam and single beam. Fig. 7 shows an example of the ground-truth RRIs, the RRIs estimated with a single beam, and the RRIs estimated with multibeam. In this figure, we use 0° as the single beam. From this figure, it can be seen that the Viterbi algorithm roughly can track the actual RRIs by using multibeam. In addition, Fig. 8 shows the peaks detected between 20 s and 30 s for the same subject. In this figure, we can see that the number of peak candidates close to the true timing increases by using multibeam. As a result, through the Viterbi algorithm, the detected peaks with multibeam are more accurate than those with a single beam. Furthermore, Fig. 7 shows that

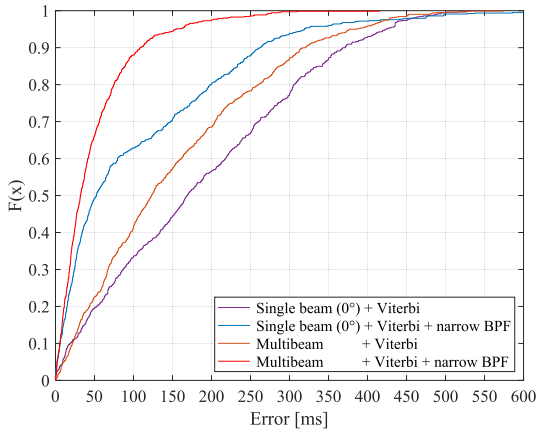

(i) CDF of all the subjects at the measurement distance of 0.6 m.

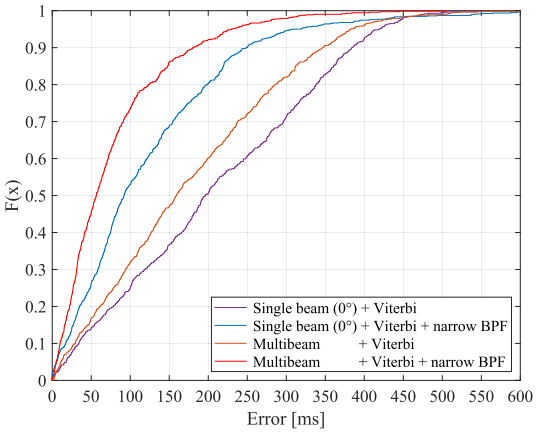

(ii) CDF of all the subjects at the measurement distance of 1.0 m.

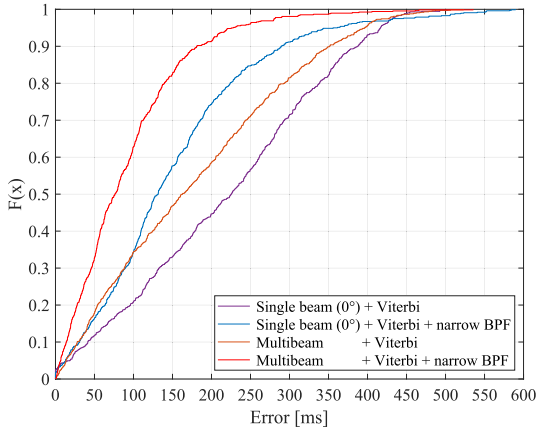

(iii) CDF of all the subjects at the measurement distance of 2.0 m.

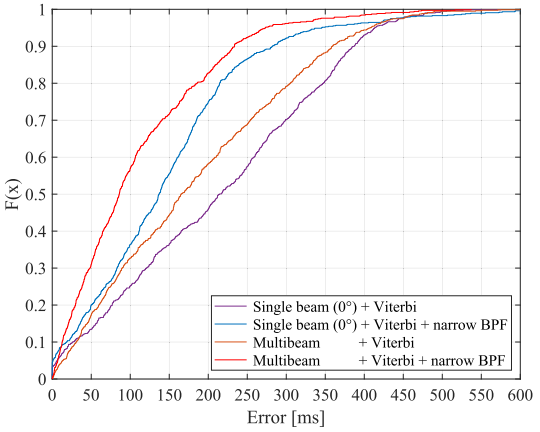

(iv) CDF of all the subjects at the measurement distance of 3.0 m.

FIGURE 9. CDF of all the subjects at different measurement distances of (i) 0.6 m (ii) 1.0 m (iii) 2.0 m, and (iv) 3.0 m, by the proposed method in four cases, which are the Viterbi algorithm and the Viterbi algorithm and narrow BPF when using the single beam of 0°, and the Viterbi algorithm and the Viterbi algorithm and narrow BPF when using the proposed method.

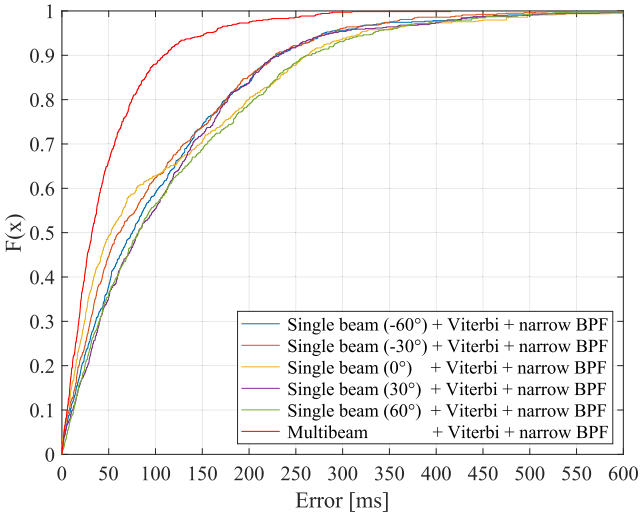

FIGURE 10. CDF of all the subjects of the proposed methods that use multibeam and a single beam at the measurement distance of 0.6 m.

by applying the narrow BPF, we can estimate the RRI more accurately. The RRI estimation accuracy of the proposed method with multibeam is evident compared to the method with the single beam.

Fig. 9 shows CDFs of all the subjects at the different measurement distances, i.e., (i) 0.6 m (ii) 1.0 m (iii) 2.0 m, and (iv) 3.0 m. This figure shows that the proposed method using multibeam estimates RRI more accurately than the proposed method using the single beam of 0° at all the distances. In particular, when using a single beam, the percentages of the errors less than 100 ms at 0.6 m, 0.1 m, 0.2 m, and 0.3 m are 41%, 33%, 35%, and 33%, respectively, while, those of our proposal are 88%, 73%, 63%, and 56%, respectively.

TABLE 5 lists the performance comparison of the proposed methods that use multibeam and a single beam. In this table, 13 beam directions, i.e., −60°, −50°, −40°, …, 60°, are shown as a single beam direction. As can be seen from this table, the proposed method using multibeam significantly improves the AE and the RMSE of the methods using a single beam for 0.6 m: The average RMSE of the methods using a single beam is 140 ms, while that of our proposal is 63 ms. In addition, even when the detection range is long, i.e., 1.0 m,

TABLE 6. RRI accuracy comparison of the conventional methods and the proposed method∗ at different measurement distances *d*.

$d\ [m]$	RMSE [ms]			
	[41]	[47]	[48]	Proposal
0.6	94	265	386	63
1.0	131	248	475	103
2.0	152	262	499	118
3.0	189	271	518	138
Ave.	142	265	469	105

∗ The proposed method uses the beam interval between adjacent directions θ_b of $5°$, the time interval T_c of 30 s and the threshold th_c of 0.9.

2.0 m, and 3.0 m, our proposed method using multibeam outperforms the methods using a single beam for any beam directions by both the AE and the RMSE. As a result, our method achieves the RMSE of 137 ms for the detection range of 3.0 m. This result is worth noting, considering that the average RMSE of the methods using a single beam is 140 ms even for 0.6 m. Fig. 10 shows the CDF of all the subjects of the proposed methods that use multibeam and a single beam, i.e., $-60°$, $-30°$, $0°$, $30°$, and $60°$, at the measurement distance of 0.6 m. From this figure, it can be seen that the accuracy was greatly improved by using multibeam. In particular, the percentage of the errors less than 100 ms by the method using a single beam is 60%, while that of our proposal is 88%. These results indicate that using beam diversity can lead to the improvement of the heartbeat detection accuracy.

D. PERFORMANCE COMPARISON BETWEEN THE PROPOSED METHOD AND THE CONVENTIONAL METHODS

To further validate the performance of the proposed method, we compared our proposed method with the conventional methods [41], [47], [48] that estimate the RRI. For the conventional methods, the average of the in-phase and quadrature signals $I_k(t)$ and $Q_k(t)$, $k = 1, \ldots, 4$, obtained by the four receive antennas is used. TABLE 6 shows the RMSEs at the distances of 0.6 m, 1.0 m, 2.0 m, and 3.0 m. As can be seen from this table, the proposed method provides the lowest RMSE for all the distances. In the conventional methods [41], [47], [48], the estimation accuracy significantly degrades, regardless of the measurement distance. This is due to detecting false peaks and missing true peaks caused by the degradation of the SNR of heartbeat components. The results of these conventional methods show that the heartbeat detection accuracy can be significantly affected by noise when using only a single beam. Based on these results, it is clear that using multibeam can lead to accurate heartbeat detection, compared to using a single beam.

VI. CONCLUSION

In this paper, we proposed the heartbeat detection method based on beam diversity using a multibeam Doppler sensor. In contrast to the conventional methods that use a signal beam, the proposed method takes advantage of multibeam to detect heartbeat accurately. Based on the fact that the SNR of heartbeat components is different from one beam to another, the proposed method extracts heartbeat components from all peaks detected by the multi-beam signals. Through the experiments, we showed that our proposed method improved the RMSE of the methods using a single beam. Also, through the performance evaluation of our proposed method for different parameter settings, we showed the parameter settings that could provide accurate heartbeat detection. These experimental results validate our proposed method and indicate that utilizing beam diversity is effective in improving the heartbeat detection accuracy. In the future, for cases where the subject's state is not static, we would like to conduct additional experiments and examine how much our method is robust to such a case.

REFERENCES

[1] C. G. Caro and J. A. Bloice, "Contactless apnoea detector based on radar," *Lancet*, vol. 298, pp. 959–961, Oct. 1971.

[2] C. I. Franks, B. H. Brown, and D. M. Johnston, "Contactless respiration monitoring of infants," *Med. Biol. Eng.*, vol. 14, no. 3, pp. 306–312, May 1976.

[3] C. Li, V. M. Lubecke, O. Boric-Lubecke, and J. Lin, "A review on recent advances in Doppler radar sensors for noncontact healthcare monitoring," *IEEE Trans. Microw. Theory Techn.*, vol. 61, no. 5, pp. 2046–2060, May 2013.

[4] J. Wang, X. Wang, Z. Zhu, J. Huangfu, C. Li, and L. Ran, "1-D microwave imaging of human cardiac motion: An ab-initio investigation," *IEEE Trans. Microw. Theory Techn.*, vol. 61, no. 5, pp. 2101–2107, May 2013.

[5] W. Massagram, V. M. Lubecke, A. Høst-Madsen, and O. Boric-Lubecke, "Assessment of heart rate variability and respiratory sinus arrhythmia via Doppler radar," *IEEE Trans. Microw. Theory Techn.*, vol. 57, no. 10, pp. 2542–2549, Oct. 2009.

[6] C. Li, J. Lin, and Y. Xiao, "Robust overnight monitoring of human vital signs by a non-contact respiration and heartbeat detector," in *Proc. Int. Conf. IEEE Eng. Med. Biol. Soc.*, Aug. 2006, pp. 2235–2238.

[7] J.-S. Wong, W.-A. Lu, K.-T. Wu, M. Liu, G.-Y. Chen, and C.-D. Kuo, "A comparative study of pulse rate variability and heart rate variability in healthy subjects," *J. Clin. Monit. Comput.*, vol. 26, no. 2, pp. 107–114, Apr. 2012.

[8] A. Hernando, J. Lazaro, E. Gil, A. Arza, J. M. Garzon, R. Lopez-Anton, C. de la Camara, P. Laguna, J. Aguilo, and R. Bailon, "Inclusion of respiratory frequency information in heart rate variability analysis for stress assessment," *IEEE J. Biomed. Health Informat.*, vol. 20, no. 4, pp. 1016–1025, Jul. 2016.

[9] M. Ambrosanio, S. Franceschini, G. Grassini, and F. Baselice, "A multi-channel ultrasound system for non-contact heart rate monitoring," *IEEE Sensors J.*, vol. 20, no. 4, pp. 2064–2074, Feb. 2020.

[10] S. Franceschini, M. Ambrosanio, and F. Baselice, "MUHD: A multi-channel ultrasound prototype for remote heartbeat detection," in *BIODEVICES*. SciTePress, 2020, pp. 57–63.

[11] M. Rehman, R. A. Shah, M. B. Khan, N. A. A. Ali, A. A. Alotaibi, T. Althobaiti, N. Ramzan, S. A. Shah, X. Yang, A. Alomainy, M. A. Imran, and Q. H. Abbasi, "Contactless small-scale movement monitoring system using software defined radio for early diagnosis of COVID-19," *IEEE Sensors J.*, vol. 21, no. 15, pp. 17180–17188, Aug. 2021.

[12] E. L. Chuma and Y. Iano, "A movement detection system using continuous-wave Doppler radar sensor and convolutional neural network to detect cough and other gestures," *IEEE Sensors J.*, vol. 21, no. 3, pp. 2921–2928, Feb. 2021.

[13] M. Ali, A. Elsayed, A. Mendez, Y. Savaria, M. Sawan, and M. Sawan, "Contact and remote breathing rate monitoring techniques: A review," *IEEE Sensors J.*, vol. 21, no. 13, pp. 14569–14586, Jul. 2021.

[14] C. Gu, C. Li, J. Lin, J. Long, J. Huangfu, and L. Ran, "Instrument-based noncontact Doppler radar vital sign detection system using heterodyne digital quadrature demodulation architecture," *IEEE Trans. Instrum. Meas.*, vol. 59, no. 6, pp. 1580–1588, Jun. 2010.

[15] G. Vinci, S. Lindner, F. Barbon, S. Mann, M. Hofmann, A. Duda, and A. Koelpin, "Six-port radar sensor for remote respiration rate and heartbeat vital-sign monitoring," *IEEE Trans. Microw. Theory Techn.*, vol. 61, no. 5, pp. 2093–2100, May 2013.

[16] İ. Güler, F. Hardalaç, and N. Barşçı, "Application of FFT analyzed cardiac Doppler signals to fuzzy algorithm," *Comput. Biol. Med.*, vol. 32, no. 6, pp. 435–444, Nov. 2002.

[17] J. Tu and J. Lin, "Respiration harmonics cancellation for accurate heart rate measurement in non-contact vital sign detection," in *IEEE MTT-S Int. Microw. Symp. Dig.*, Jun. 2013, pp. 1–3.

[18] J. Tu and J. Lin, "Fast acquisition of heart rate in noncontact vital sign Radar measurement using time-window-variation technique," *IEEE Trans. Instrum. Meas.*, vol. 65, no. 1, pp. 112–122, Jan. 2016.

[19] A. Tariq and H. G. Shiraz, "Doppler radar vital signs monitoring using wavelet transform," in *Proc. Loughborough Antennas Propag. Conf.*, Nov. 2010, pp. 293–296.

[20] M. Sekine and K. Maeno, "Non-contact heart rate detection using periodic variation in Doppler frequency," in *Proc. IEEE Sensors Appl. Symp.*, Feb. 2011, pp. 318–322.

[21] A. Tariq and H. Ghafouri-Shiraz, "Vital signs detection using Doppler radar and continuous wavelet transform," in *Proc. 5th Eur. Conf. Antennas Propag.*, Apr. 2015, pp. 285–288.

[22] M. He, Y. Nian, and B. Liu, "Noncontact heart beat signal extraction based on wavelet transform," in *Proc. 8th Int. Conf. Biomed. Eng. Inform. (BMEI)*, Shenyang, China, Oct. 2015, pp. 209–213.

[23] M. Li and J. Lin, "Wavelet-transform-based data-length-variation technique for fast heart rate detection using 5.8-GHz CW Doppler radar," *IEEE Trans. Microw. Theory Techn.*, vol. 66, no. 1, pp. 568–576, Jan. 2018.

[24] P. Bechet, R. Mitran, and M. Munteanu, "A non-contact method based on multiple signal classification algorithm to reduce the measurement time for accurately heart rate detection," *Rev. Scientific Instrum.*, vol. 84, no. 8, Aug. 2013, Art. no. 084707.

[25] K. J. Lee, C. Park, and B. Lee, "Tracking driver's heart rate by continuous-wave Doppler radar," in *Proc. IEEE Eng. Med. Biol. Soc. (EMBC)*, Aug. 2016, pp. 5417–5420.

[26] K. Yamamoto, K. Toyoda, and T. Ohtsuki, "Non-contact heartbeat detection by MUSIC with discrete cosine transform-based parameter adjustment," in *Proc. IEEE Global Commun. Conf. (GLOBECOM)*, Dec. 2018, pp. 1–6.

[27] K. Yamamoto, K. Toyoda, and T. Ohtsuki, "MUSIC-based Non-contact heart rate estimation with adaptive window size setting," in *Proc. IEEE Eng. Med. Biol. Soc. (EMBC)*, Jul. 2019, pp. 6073–6076.

[28] J. Park, J.-W. Ham, S. Park, D.-H. Kim, S.-J. Park, H. Kang, and S.-O. Park, "Polyphase-basis discrete cosine transform for real-time measurement of heart rate with CW Doppler radar," *IEEE Trans. Microw. Theory Techn.*, vol. 66, no. 3, pp. 1644–1659, Mar. 2018.

[29] M. Nosrati and N. Tavassolian, "High-accuracy heart rate variability monitoring using Doppler radar based on Gaussian pulse train modeling and FTPR algorithm," *IEEE Trans. Microw. Theory Techn.*, vol. 66, no. 1, pp. 556–567, Jan. 2018.

[30] Y. Wan, X. Liang, X. Bu, and Y. Liu, "FOD detection method based on iterative adaptive approach for millimeter-wave radar," *Sensors*, vol. 21, no. 4, p. 1241, Feb. 2021.

[31] Y. Zhang, J. Luo, J. Li, D. Mao, Y. Zhang, Y. Huang, and J. Yang, "Fast inverse-scattering reconstruction for airborne high-squint radar imagery based on Doppler centroid compensation," *IEEE Trans. Geosci. Remote Sens.*, vol. 60, pp. 1–17, 2022.

[32] C. Will, K. Shi, F. Lurz, R. Weigel, and A. Koelpin, "Instantaneous heartbeat detection using a cross-correlation based template matching for continuous wave radar systems," in *Proc. IEEE Topical Conf. Wireless Sensors Sensor Netw. (WiSNet)*, Jan. 2016, pp. 31–34.

[33] C. Will, K. Shi, R. Weigel, and A. Koelpin, "Advanced template matching algorithm for instantaneous heartbeat detection using continuous wave radar systems," in *IEEE MTT-S Int. Microw. Symp. Dig.*, May 2017, pp. 1–4.

[34] S. Bounyong, M. Yoshioka, and J. Ozawa, "Monitoring of a driver's heart rate using a microwave sensor and template-matching algorithm," in *Proc. IEEE Int. Conf. Consum. Electron. (ICCE)*, Jan. 2017, pp. 43–44.

[35] S. Izumi, T. Okano, D. Matsunaga, H. Kawaguchi, and M. Yoshimoto, "Non-contact instantaneous heart rate extraction system using 24-GHz microwave Doppler sensor," *IEICE Trans. Commun.*, vol. 102, no. 6, pp. 1088–1096, Jun. 2019.

[36] I. V. Mikhelson, P. Lee, S. Bakhtiari, T. W. Elmer, II, A. K. Katsaggelos, and A. V. Sahakian, "Noncontact millimeter-wave real-time detection and tracking of heart rate on an ambulatory subject," *IEEE Trans. Inf. Technol. Biomed.*, vol. 16, no. 5, pp. 927–934, Sep. 2012.

[37] T. Ohtsuki and E. Mogi, "Heartbeat detection with Doppler radar based on estimation of average R-R interval using Viterbi algorithm," in *Proc. IEEE 27th Annu. Int. Symp. Pers., Indoor, Mobile Radio Commun. (PIMRC)*, Sep. 2016, pp. 1–5.

[38] X. Yang, G. Sun, and K. Ishibashi, "Non-contact acquisition of respiration and heart rates using Doppler radar with time domain peak-detection algorithm," in *Proc. 39th Annu. Int. Conf. IEEE Eng. Med. Biol. Soc. (EMBC)*, Jul. 2017, pp. 2847–2850.

[39] J.-Y. Kim, J.-H. Park, S.-Y. Jang, and J.-R. Yang, "Peak detection algorithm for vital sign detection using Doppler radar sensors," *Sensors*, vol. 19, no. 7, p. 1575, Apr. 2019.

[40] R. Hiromatsu, K. Yamamoto, K. Toyoda, and T. Ohtsuki, "Novel CA-CFAR approach for improvement of Doppler sensor-based heart rate variability estimation," in *Proc. 41st Annu. Int. Conf. IEEE Eng. Med. Biol. Soc. (EMBC)*, Jul. 2019, pp. 796–799.

[41] K. Yamamoto and T. Ohtsuki, "Noncontact heartbeat detection by Viterbi algorithm with fusion of beat-beat interval and deep learning-driven branch metrics," in *Proc. IEEE Int. Conf. Acoust., Speech Signal Process. (ICASSP)*, Jun. 2021, pp. 8308–8312.

[42] S. Tomii and T. Ohtsuki, "Heartbeat detection by using Doppler radar with wavelet transform based on scale factor learning," in *Proc. IEEE Int. Conf. Commun.*, Jun. 2015, pp. 483–488.

[43] E. Mogi and T. Ohtsuki, "Heartbeat detection with Doppler sensor using adaptive scale factor selection on learning," in *Proc. IEEE 26th Annu. Int. Symp. Pers., Indoor, Mobile Radio Commun. (PIMRC)*, Aug. 2015, pp. 2166–2170.

[44] J. Saluja, J. Casanova, and J. Lin, "A supervised machine learning algorithm for heart-rate detection using Doppler motion-sensing radar," *IEEE J. Electromagn., RF Microw. Med. Biol.*, vol. 4, no. 1, pp. 45–51, Mar. 2020.

[45] Y. Iwata, H. T. Thanh, G. Sun, and K. Ishibashi, "High accuracy heartbeat detection from CW-Doppler radar using singular value decomposition and matched filter," *Sensors*, vol. 21, no. 11, p. 3588, May 2021.

[46] T. Sakamoto, R. Imasaka, H. Taki, T. Sato, M. Yoshioka, K. Inoue, and H. Sakai, "Feature-based correlation and topological similarity for interbeat interval estimation using ultrawideband radar," *IEEE Trans. Biomed. Eng.*, vol. 63, no. 4, pp. 747–757, Apr. 2016.

[47] W. Hu, Z. Zhao, Y. Wang, H. Zhang, and F. Lin, "Noncontact accurate measurement of cardiopulmonary activity using a compact quadrature Doppler radar sensor," *IEEE Trans. Biomed. Eng.*, vol. 61, no. 3, pp. 725–735, Mar. 2014.

[48] V. L. Petrović, M. M. Janković, A. V. Lupšić, V. R. Mihajlović, and J. S. Popović-Bovović, "High-accuracy real-time monitoring of heart rate variability using 24 GHz continuous-wave Doppler radar," *IEEE Access*, vol. 7, pp. 74721–74733, 2019.

[49] K. Yamamoto, K. Toyoda, and T. Ohtsuki, "Spectrogram-based non-contact RRI estimation by accurate peak detection algorithm," *IEEE Access*, vol. 6, pp. 60369–60379, 2018.

[50] T. Kitagawa, K. Yamamoto, and T. Ohtsuki, "Non-contact heartbeat detection based on beam diversity using multibeam Doppler sensor," in *Proc. IEEE Global Commun. Conf. (GLOBECOM)*, Dec. 2021, pp. 1–6.

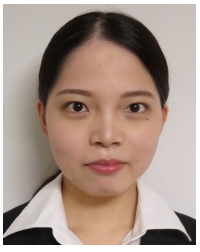

TSUKIKO KITAGAWA (Graduate Student Member, IEEE) was born in Okayama, Japan, in1998. She received the B.E. degree from the Faculty of Science and Technology, Keio University, in 2021. She is currently pursuing the master's degree with the Graduate School of Science and Technology, Keio University. Her research interest includes signal processing. She is a member of IEICE.

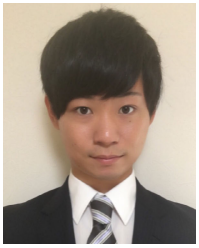

KOHEI YAMAMOTO (Student Member, IEEE) was born in Kanagawa, Japan, in1994. He received the B.E. and M.E. degrees from the Faculty of Science and Technology, Keio University, in 2017 and 2019, respectively. He is currently pursuing the Ph.D. degree with the Graduate School of Science and Technology, Keio University. His research interest includes signal processing. He is a member of IEICE.

KOJI ENDO (Member, IEEE) was born in Gifu, Japan, in 1984. He received the B.E. degree from the Nagoya Institute of Technology, Nagoya, Japan, and the M.E. degree from Nagoya University, Nagoya, in 2006 and 2008, respectively. In 2008, he joined the Technical Research and Development Institute, Ministry of Defense, Japan, where he was engaged in the research of RF sensor systems. He is currently pursuing the Ph.D. degree with the Graduate School of Science and Technology, Keio University. His research interest includes array signal processing. He is a member of IEICE.

TOMOAKI OHTSUKI (Senior Member, IEEE) received the B.E., M.E., and Ph.D. degrees in electrical engineering from Keio University, Yokohama, Japan, in 1990, 1992, and 1994, respectively. From 1993 to 1995, he was a Special Researcher of Fellowships at the Japan Society for the Promotion of Science for Japanese Junior Scientists. From 1994 to 1995, he was a Postdoctoral Fellow and a Visiting Researcher of electrical engineering at Keio University. From 1995 to 2005, he was with the Tokyo University of Science. From 1998 to 1999, he was with the Department of Electrical Engineering and Computer Sciences, University of California at Berkeley. In 2005, he joined Keio University, where he is currently a Professor. He has published more than 215 journal articles and 420 international conference papers. His research interests include wireless communications, optical communications, signal processing, and information theory. He was a recipient of the 1997 Inoue Research Award for Young Scientist, the 1997 Hiroshi Ando Memorial Young Engineering Award, the Ericsson Young Scientist Award 2000, the 2002 Funai Information and Science Award for Young Scientist, IEEE the First Asia–Pacific Young Researcher Award 2001, the 5th International Communication Foundation (ICF) Research Award, the 2011 IEEE SPCE Outstanding Service Award, the 27th TELECOM System Technology Award, the ETRI Journal's 2012 Best Reviewer Award, and the 9th International Conference on Communications and Networking in China 2014 (CHINACOM '14) Best Paper Award. He was the Chair of IEEE Communications Society, Signal Processing for Communications, and Electronics Technical Committee. He served as a Technical Editor for *IEEE Wireless Communications Magazine* and an Editor for *Elsevier Physical Communications*. He is currently serving as an Area Editor for the IEEE TRANSACTIONS ON VEHICULAR TECHNOLOGY and an Editor of the IEEE COMMUNICATIONS SURVEYS AND TUTORIALS. He has served as a General Co-Chair, a Symposium Co-Chair, and a TPC Co-Chair for many conferences, including IEEE GLOBECOM 2008, SPC, IEEE ICC 2011, CTS, IEEE GLOBECOM 2012, SPC, IEEE ICC 2020, SPC, IEEE APWCS, IEEE SPAWC, and IEEE VTC. He gave tutorials and keynote speeches at many international conferences, including IEEE VTC, IEEE PIMRC, and IEEE WCNC. He was a Vice President and the President of the Communications Society of the IEICE. He is a Distinguished Lecturer of the IEEE, a fellow of the IEICE, and a member of the Engineering Academy of Japan.